Climate simulation of the latest Permian: Implications for mass extinction

Jeffrey T. Kiehl*
Christine A. Shields*
Climate Change Research Section, National Center for Atmospheric Research, 1850 Table Mesa Drive, Boulder, Colorado 80305, USA

ABSTRACT

Life at the Permian-Triassic boundary (ca. 251 Ma) underwent the largest disruption in Earth's history. Paleoclimatic data indicate that Earth was significantly warmer than present and that much of the ocean was anoxic or euxinic for an extended period of time. We present results from the first fully coupled comprehensive climate model using paleogeography for this time period. The coupled climate system model simulates warm high-latitude surface air temperatures related to elevated carbon dioxide levels and a stagnate global ocean circulation in concert with paleodata indicating low oxygen levels at ocean depth. This is the first climate simulation that captures these observed features of this time period.

Keywords: Permian-Triassic boundary, mass extinctions, ocean circulation, anoxia.

INTRODUCTION

We present results from a comprehensive climate system model that indicate that elevated levels of CO_2 during the latest Permian led to climatic conditions inhospitable to both marine and terrestrial life. The largest extinction in Earth's history took place 251 Ma, at the Permian-Triassic boundary (e.g., Erwin, 1993). Over the past 20 yr a number of hypotheses have been put forward to explain this extinction event (Erwin et al., 2002; Benton and Twitchett, 2003). The paleoclimatic data indicate that this was a time of warm surface temperatures, especially in high-latitude polar regions (Retallack, 1995; Chumakov and Zharkov, 2003). Several studies indicate that the oceans at this time were either anoxic or euxinic for an extended period of time (e.g., Wignall and Twitchett, 1996). Approximately 90%–95% of life was extinguished in the oceans, and there was a significant loss of terrestrial life (~70%). One factor that has been quantified is the presence of large magmatic flows, the Siberian Traps, coincident in time with the development of these disruptions in life forms (Renne et al., 1995). This volcanic activity, which lasted for ~700 k.y., would have released significant amounts of carbon dioxide and sulfur dioxide into the atmosphere. There is also the possibility of a large injection of methane into the atmosphere through the destabilization of clathrates, which could explain the excursion in $\delta^{13}C$ at this time (Erwin, 1993; Berner, 2002). The challenge for any climate model simulation of this time period is to simulate a climate in concert with the geological, palentological, and geochemical data. To date this has proven difficult to accomplish with uncoupled climate models (Kutzbach and Ziegler, 1993; Rees et al., 1999).

MODEL DESCRIPTION

Previous modeling studies include uncoupled ocean models forced with prescribed surface boundary conditions (Hotinski et al., 2001; Zhang et al., 2001), the coupling of an energy balance model to an ocean model (Winguth et al., 2002), and more recently using a simplified atmosphere model coupled to an ocean model with idealized boundary conditions (Smith and Dubois, 2004). To date no fully comprehensive coupled atmosphere, land, ocean, and sea-ice system model using realistic geography and topography has been used to study the climate of the Permian-Triassic boundary. We present results from such a comprehensive model with realistic boundary conditions. The model used is the latest version of the Community Climate System Model (CCSM3). The model used for this study employs a T31 (3.75° × 3.75°) horizontal resolution version for the atmosphere and a nominal 3° ocean model with 25 levels. This lower resolution version of the CCSM3 yields a realistic simulation of the present climate, where the present-day control simulation has been run for ~900 yr and the energy balance of the system is -0.05 Wm^{-2}, i.e., the control climate is in near steady state. The ocean circulation is in very good agreement with observational data, e.g., the simulated strength of the North Atlantic meridional overturning circulation is 16 Sv, in good agreement with the observed strength of 15–23 Sv, where 1 Sv = 10^6 m^3 s^{-1}.

The boundary conditions for the latest Permian simulations employ paleogeography and paleotopography for this time period (provided by D. Rowley, 2005, personal commun.). The ocean bathymetry for the deep ocean is a flat bottom condition. Land surface albedos were based on the surface types of Rees et al. (1999), where the warm temperate regions were expanded to higher latitudes. The CCSM3 land model generates surface albedos from the prescribed surface types. The atmospheric composition is a key unknown for this time period, especially with regard to levels of atmospheric carbon dioxide. The presence of elevated methane levels has also been postulated for this time period. Based on work of Kidder and Worsley (2004), the CO_2 level for the climate simulation is set to 10 times the present concentration. This yields an initial radiative forcing of 14.5 Wm^{-2}. Note that even higher levels of CO_2 have been proposed for this time period (Kidder and Worsley, 2004), thus a tenfold increase in CO_2 is viewed as a conservative estimate of the atmospheric CO_2 at the Permian-Triassic boundary. A summary of the latest Permian model boundary conditions is in Table 1.

Given these boundary conditions, the fully coupled CCSM3 is initialized with global mean ocean temperatures from a warm Cretaceous climate simulation (Otto-Bliesner et al., 2002), and no sea ice and a uniform salinity of 35 practical salinity units. The climate model has been run for 2700 yr to an equilibrium state, which is determined by considering the net flux of energy into the climate system and the trend in deep ocean overturning circulation. The net energy flux into the system averaged over the last 100 yr of the simulation is -0.03 Wm^{-2} compared to the control imbalance of -0.05 Wm^{-2}, indicating that both the present-day control and latest Permian simulations are in energy balance. Trends in the strength of the deep ocean over-

TABLE 1. BOUNDARY CONDITIONS FOR THE LATEST PERMIAN SIMULATION

	CO_2 (ppmv)	CH_4 (ppmv)	N_2O (ppmv)	S_0 (Wm^{-2})	Eccentricity	Obliquity (Degrees)
Value	3550	0.7	0.275	1338	0	23.5

Note: ppmv is parts per million by volume.

*E-mails: jtkon@ucar.edu; shields@ucar.edu.

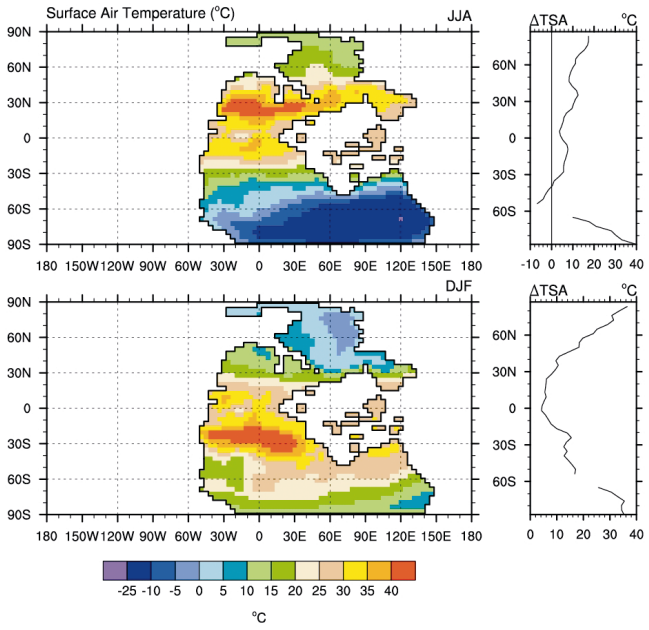

Figure 1. Simulated seasonal mean surface air temperatures (°C) from fully coupled latest Permian climate simulation. Top panel: June-July-August; bottom panel: December-January February. Side panels show zonal mean difference of surface air temperature (TSA) from control simulation for two respective seasons.

turning circulation are <0.002 Sv/100 yr in the last 300 yr of the integration. All results are based on an average of the last 100 yr of the simulation. The latest Permian global mean surface temperature is 7.98 °C warmer than present day.

RESULTS

Terrestrial Simulation

A common problem with previous Permian simulations, employing fourfold to eightfold increases in CO_2 levels, is extremely cold land surface temperatures at high latitudes, inconsistent with paleopalynological and paleosol data (Retallack et al., 2003; Taylor et al., 1992), where the data indicate the existence of deciduous forests at high latitudes. Our simulated near-surface temperatures for winter and summer seasons are shown in Figure 1. The lowest seasonal mean temperature from the latest Permian simulation is in Southern Hemisphere winter with a value of −23 °C; over much of this region surface air temperatures are considerably higher than previous climate simulations. We have carried out a parallel latest Permian simulation with present levels of CO_2 to determine whether it is the higher CO_2 or paleogeography that contributes most to this polar warming. The latest Permian simulation with present level CO_2 yields annual mean zonal mean polar land temperatures that are below the freezing level, although these temperatures are warmer than the present-day simulation. This polar warming relative to present day is related to open ocean areas that allow for poleward heat transport that is not possible with present geography (e.g., Greenland and Antarctica). We conclude from the comparison of these simulations that elevated CO_2 is the dominant reason for the warm polar regions, and that the existence of ocean heat transport poleward of ~60° north and south contributes to additional warming, as do lower surface albedos due to the lack of permanent land ice.

Surface air temperatures are 10–40 °C warmer than the present-day control simulation at the highest southern latitudes (see Fig. 1, sidebar). In the Northern Hemisphere winter land temperatures are 10–20 °C warmer than the present-day simulation and are more consistent with the paleoclimatic data. For example, Retallack et al. (2003) argued that temperatures in the Karoo Basin region were ~9–10 °C in the latest Permian, in agreement with the annual mean temperatures simulated by the model for this region. Mean precipitation was ~1–2 mmd^{-1}, where the model simulates 1.5 mmd^{-1}. The minimum daily mean maximum summer temperatures in the dry subtropical regions are 51 °C in some regions, which is 15 °C higher than simulated present-day daily maximum summer temperatures. These extreme daily temperature maxima in these regions would contribute to a decrease in terrestrial flora and fauna.

Ocean Simulation

Paleodata indicate that sea surface temperatures were much warmer in the Late Permian (Holser et al., 1989). Figure 2 shows the annual mean sea surface temperatures for the Late Permian simulation, while the side panel indicates the difference in zonal mean sea surface temperatures compared to the present-day control. Over the high-latitude northern and southern Panthalassic Ocean regions much of the ocean surface is 8 °C, substantially warmer than present-day sea surface temperatures, which are near 0 °C at these high-latitude regions. This warm water persists to depth; at 3000 m the water is 4.5–5 °C, compared to present-day temperatures that are near freezing. Note that Late Permian equatorial sea surface temperatures are not substantially warmer compared to present-day equatorial waters. There appears to be a strong regulation of tropical ocean temperatures in this coupled simulation. The simulated spatial distribution of tropical sea surface temperatures is similar to present day with a warm pool of water forming in the tropical eastern Tethys and western Panthalassic, and a cold tongue of water in the eastern tropical Panthalassic Ocean caused by upwelling in this region.

Globally the latest Permian oceans are 4 °C warmer than the present-day ocean and in good agreement with the paleodata (Holser et al., 1989; Kidder and Worsley, 2004). The Late Permian ocean is also more saline than present day; at depths of 3000 m, the salinity is greater by ~1.5 practical salinity units. This

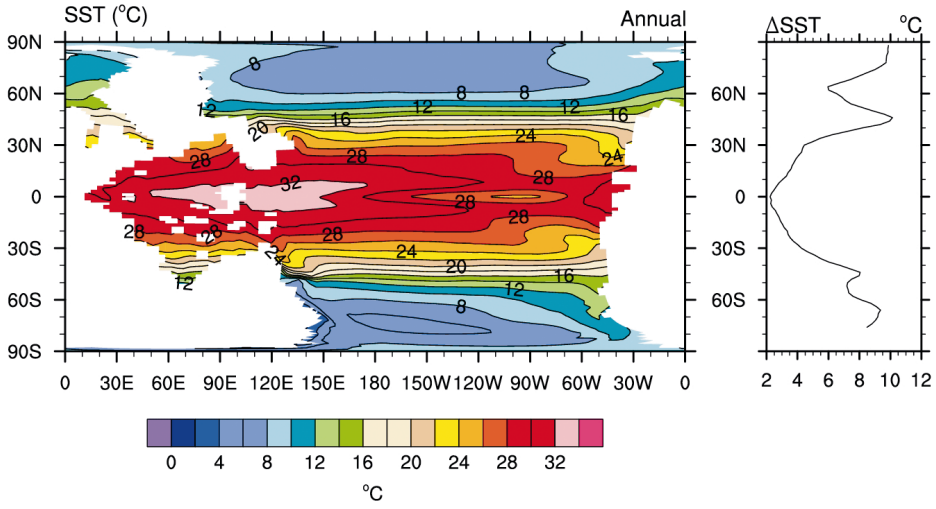

Figure 2. Simulated latest Permian annual mean sea surface temperatures (SSTs, °C). Side panel shows difference of zonal mean Permian SSTs from present-day simulated SSTs.

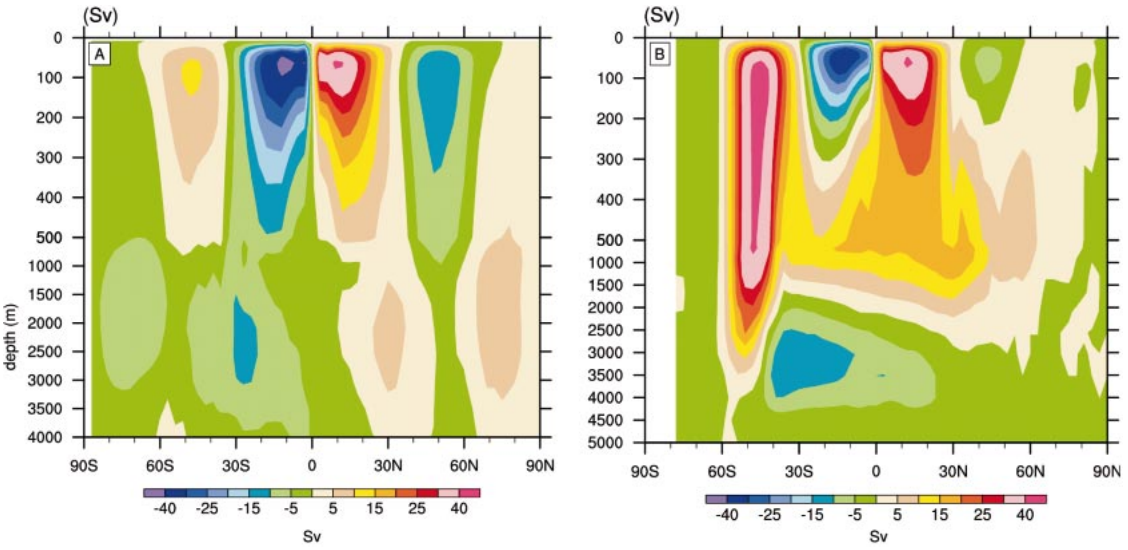

Figure 3. Simulated zonal mean meridional overturning circulation (Sv) in latest Permian simulation (A) and present-day simulation (B). 1 Sv = 10^6 m^3s^{-1}.

simulated deep warm saline water also agrees with paleodata for this time period.

Ocean Circulation and Implications for Anoxia

The simulated, more stable, potential density structure of the latest Permian ocean is consistent with a weak overturning circulation, which has significant implications for ocean mixing. In particular, the Tethys Sea is extremely stratified due to limited connection with the larger Panthalassic Ocean. One measure of the level of stratification is the strength of the meridional overturning circulation, as shown in Figure 3.

In the present day, deep-water formation occurs off Greenland and Antarctica due to the formation of cold dense saline water, which sinks to depth. The latest Permian simulation from the coupled model does not exhibit this type of mixing to depth. There is little deep-water formation due to the warm, less dense waters at high latitudes in both hemispheres. The overturning circulation of the latest Permian at depth is symmetric about the equator with a weak strength of ~10 Sv. This solution contrasts with uncoupled simulations and a more recent coupled model using simplified geographic boundary conditions and present-day CO_2 levels. The uncoupled ocean models need to be forced with either fluxes or surface air state information. These forcings of momentum, energy, and freshwater input are fixed in time. Thus, as the ocean climate comes into a new equilibrium there is no feedback with atmospheric and hydrologic processes.

What are the implications of the weak ocean circulation for anoxic or euxinic conditions at depth? For the present-day climate, the pathway for oxygen to reach the deep ocean occurs at the high latitudes where dense waters sink. This enables an efficient way for water masses at depth to be exposed to the

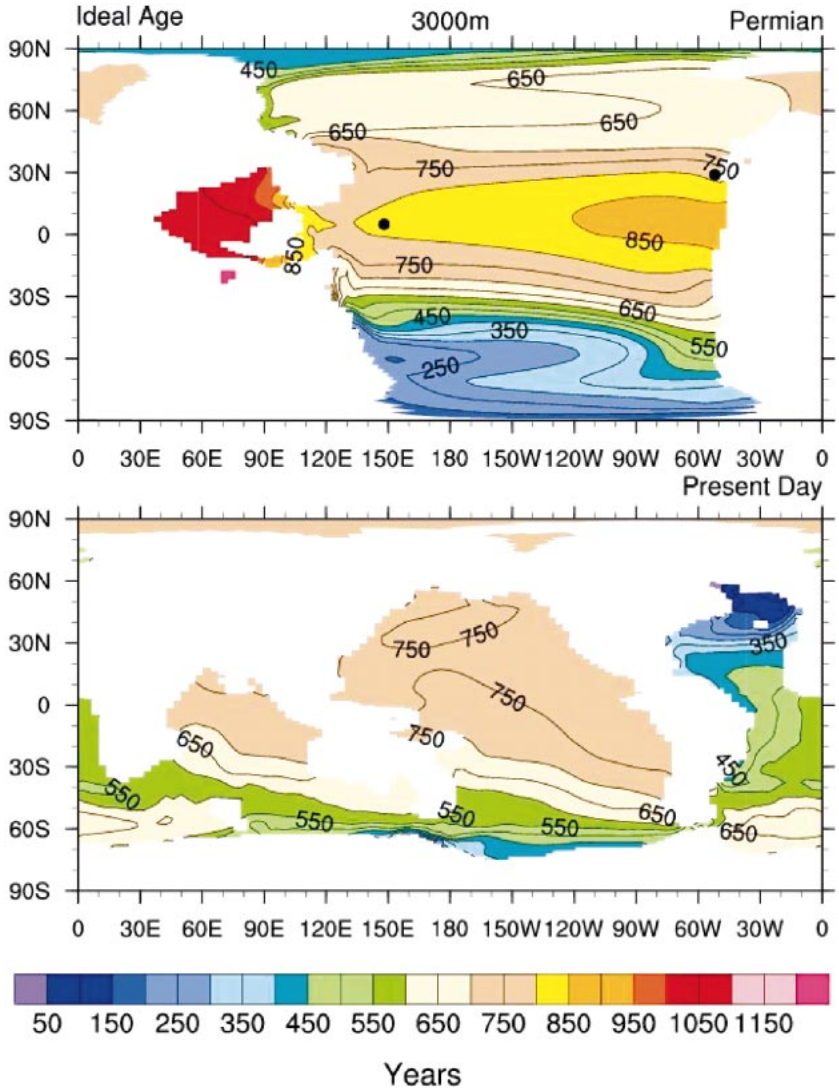

Figure 4. Simulated ideal age (years) of ocean water at 3000 m depth. Top panel is for latest Permian simulation, bottom panel is for present-day simulation. Geography is determined by bathymetry at 3000 m depth. Solid dots denote locations of paleodata.

surface. A measure of this mixing process is the ideal age, which is the time in years that a water mass at a particular depth has last been near the surface: the larger the ideal age, the less efficient the ocean mixing. The ideal age at a depth of 3000 m for the latest Permian simulation and the present-day simulation is shown in Figure 4. The ideal age is greatest for water in the Tethys Sea where the age exceeds 1000 yr. A number of recent studies focused on ocean anoxia and/or euxinia in the south Tethys and found strong evidence for little mixing in these regions (Grice et al., 2005). The latest Permian simulation supports these observational data. Indications of more extensive anoxia (Isozaki, 1997; Wang et al., 1994) come from two regions located in the tropical Panthalassic Ocean (noted by the dots in the plot in Fig. 4), which are regions of simulated long ideal ages (>800 yr). Thus, the fully coupled simulation indicates that large-scale anoxic or euxinic conditions would exist during the latest Permian–Early Triassic time period. Even at high latitudes, where in the present-day North Atlantic Ocean efficient mixing occurs (ideal age <50 yr), there is little mixing in the latest Permian. The warm, less-dense water of this time period suppresses deep-water formation, unlike the present-day situation. The implication of the latest Permian simulation is that transport of surface oxygen and nutrients to the deep ocean was very inefficient. Coupled with warmer ocean water leading to lower solubility of oxygen and lower atmospheric oxygen levels (Wignall and Twitchett, 1996; Hallam and Twitchett, 1997; Hotinski et al., 2001; Berner, 1999), this set the stage for pervasive long-term anoxia or euxinia leading to large-scale die off of marine life forms.

CONCLUSIONS

The fundamental conclusion of this study is that, given elevated CO_2 levels with realistic latest Permian paleoclimatic boundary conditions, a fully coupled comprehensive climate system model can simulate terrestrial and ocean conditions in concert with latest Permian paleodata. The implication of our study is that elevated CO_2 is sufficient to lead to inhospitable conditions for marine life and excessively high temperatures over land would contribute to the demise of terrestrial life (Ward et al., 2005). The isotopic data indicate that through the latest Permian the climate was slowly warming and $\delta^{13}C$ was decreasing, and that these changes accelerated considerably at the Permian-Triassic boundary. Given the sensitivity of ocean circulation to high-latitude warming, it is hypothesized that some critical level of high-latitude warming was reached where connection of surface waters to the deep ocean was dramatically reduced, thus leading to a shutdown of marine biologic activity, which in turn would have led to increased atmospheric CO_2 and accelerated warming.

The Siberian Traps most likely also emitted large amounts of sulfur compounds into the atmosphere. The presence of elevated levels of sulfur dioxide and methane would have contributed to the extinction of terrestrial life forms (Campbell et al., 1992; Ryskin, 2003).

ACKNOWLEDGMENTS

We thank William Large for a number of discussions on the ocean simulation. This work also benefited from conversations with Matt Huber, Steve Yeager, Bette Otto-Bliesner, and Caspar Ammann. We thank William Collins for obtaining the computational resources for this intensive model simulation. The National Center for Atmospheric Research is sponsored by the National Science Foundation.

REFERENCES CITED

Benton, M.J., and Twitchett, R.J., 2003, How to kill (almost) all life: The end-Permian extinction event: Trends in Ecology and Evolution, v. 18, p. 358–365.

Berner, R.A., 1999, Atmospheric oxygen over Phanerozoic time: National Academy of Sciences Proceedings, v. 96, p. 10,955–10,957.

Berner, R.A., 2002, Examination of hypotheses for the Permo-Triassic boundary extinction by carbon cycle modeling: National Academy of Sciences Proceedings, v. 99, p. 4172–4177.

Campbell, I.H., Czamanske, G.K., Fedorenko, V.A., Hill, R.I., and Stepanov, V., 1992, Synchronism of the Siberian Traps and the Permian-Triassic boundary: Science, v. 258, p. 1760–1763.

Chumakov, N.M., and Zharkov, M.A., 2003, Climate during the Permian-Triassic biosphere reorganizations. Article 2. Climate of the Late Permian and Early Triassic: General inferences: Stratigraphy and Geological Correlation, v. 11, p. 361–375.

Erwin, D.H., 1993, The great Paleozoic crisis, life and death in the Permian: New York, Columbia University Press, 327 p.

Erwin, D.H., Bowring, S.A., and Yugan, J., 2002, End-Permian mass extinctions: A review, *in* Koeberl, C., and MacLeod, K.G., eds., Catastrophic events and mass extinctions: Impacts and beyond: Geological Society of America Special Paper 356, p. 363–383.

Grice, K., Cao, C., Love, G.D., Böttcher, M.E., Twitchett, R.J., Grosjean, E., Summons, R.E., Turgeon, S.C., Dunning, W., and Jin, Y., 2005, Photic zone euxinia during the Permian-Triassic superanoxic event: Science, v. 307, p. 709.

Hallam, A., and Wignall, P.B., 1997, Mass extinctions and their aftermath: Oxford, Oxford University Press, 320 p.

Holser, W.T., Schönlaub, H.-P., Attrep, M., Jr., Boeckelmann, K., Klein, P., Magaritz, M., Orth, C.J., Fenninger, A., Jenny, C., Kralik, M., Mauritsch, H., Pak, E., Schramm, J.-M., Stattegger, K., and Schmöller, R., 1989, A unique geochemical record at the Permian/Triassic boundary: Nature, v. 337, p. 39–44.

Hotinski, R.M., Bice, K.L., Kump, L.R., Najar, R.G., and Arthur, M.A., 2001, Ocean stagnation and end-Permian anoxia: Geology, v. 29, p. 7–10.

Isozaki, Y., 1997, Permo-Triassic boundary superanoxia and stratified superocean: Records from lost deep sea: Science, v. 276, p. 235–238.

Kidder, D.L., and Worsley, T.R., 2004, Causes and consequences of extreme Permo-Triassic warming to globally equable climate and relation to the Permo-Triassic extinction and recovery: Palaeogeography, Palaeoclimatology, Palaeoecology, v. 203, p. 207–237.

Kutzback, J.E., and Ziegler, A.M., 1993, Simulation of Late Permian climate and biomes with an atmosphere-ocean model: Comparisons with observations: Royal Society of London Philosophical Transactions, Ser. B, v. 341, p. 327–340.

Otto-Bliesner, B.L., Brady, E.C., and Shields, C., 2002, Late Cretaceous ocean: Coupled simulations with the National Center for Atmospheric Research climate system model: Journal of Geophysical Research, v. 107, doi: 10.1029/2001JD000821.

Rees, P.M., Gibbs, M.T., Ziegler, A.M., Kutzbach, J.E., and Behling, P.J., 1999, Permian climates: Evaluating model predictions using global paleobotanical data: Geology, v. 27, p. 891–894.

Renne, P.R., Zichao, Z., Richards, M.A., Black, M.T., and Basu, A.R., 1995, Synchrony and causal relations between Permian-Triassic boundary crises and Siberian flood volcanism: Science, v. 269, p. 1413–1416.

Retallack, G.J., 1995, Permian-Triassic life crisis on land: Science, v. 267, p. 77–80.

Retallack, G.J., Smith, R.M.H., and Ward, P.D., 2003, Vertebrate extinction across Permian-Triassic boundary in Karoo Basin, South Africa: Geological Society of America Bulletin, v. 115, p. 1133–1152.

Ryskin, G., 2003, Methane-driven oceanic eruptions and mass extinctions: Geology, v. 31, p. 741–744.

Smith, R.S., and Dubois, C., 2004, Ocean circulation and climate in an idealized Pangean OAGCM: Geophysical Research Letters, v. 31, L18207, doi: 10.1029/2004GL020643.

Taylor, E.L., Taylor, T.N., and Cúneo, N.R., 1992, The present is not the key to the past: A polar forest from the Permian of Antarctica: Science, v. 257, p. 1675–1677.

Wang, K., Geldsetzer, H.H.J., and Krouse, H.R., 1994, Permian-Triassic extinction: Organic $\delta^{13}C$ evidence from British Columbia, Canada: Geology, v. 22, p. 580–584.

Ward, P.D., Botha, J., Buick, R., De Kock, M.O., Erwin, D.H., Garrison, G., Kirschvink, J.L., and Smith, R., 2005, Abrupt and gradual extinction among Late Permian land vertebrates in the Karoo Basin, South Africa: Science, v. 307, p. 709–714.

Wignall, P.B., and Twitchett, R.J., 1996, Oceanic anoxia and the end Permian mass extinction: Science, v. 272, p. 1155–1158.

Winguth, A.M.E., Heinze, C., Kutzbach, J.E., Maier-Reimer, E., Mikolajewicz, U., Rowley, D., Rees, A., and Ziegler, A.M., 2002, Simulated warm polar currents during the middle Permian: Paleoceanography, v. 17, 1057, doi: 10.1029/2001PA000646.

Zhang, R., Follows, M.J., Grotzinger, J.P., and Marshall, J., 2001, Could the Late Permian deep ocean have been anoxic: Paleoceanography, v. 16, p. 317–329.

Manuscript received 1 March 2005
Revised manuscript received 26 May 2005
Manuscript accepted 27 May 2005

Printed in USA